



Kinetics of Bacterial Adaptation, Growth, and Death at Didecyldimethylammonium Chloride sub-MIC Concentrations

Adrián Pedreira^{1,2}, José A. Vázquez^{2*} and Miriam R. García^{1*}

¹ Biosystems and Bioprocess Engineering (Bio2Eng), Marine Research Institute-Spanish National Research Council (IIM-CSIC), Eduardo Cabello, Vigo, Spain, ² Group of Recycling and Valorization of Waste Materials (REVAL), Marine Research Institute-Spanish National Research Council (IIM-CSIC), Eduardo Cabello, Vigo, Spain

Minimum inhibitory concentration (MIC) and minimum bactericidal concentration (MBC) are standard indexes for determining disinfection effectiveness. Nevertheless, they are static values disregarding the kinetics at sub-MIC concentrations where adaptation, growth, stationary, and death phases can be observed. The understanding of these dynamic mechanisms is crucial to designing effective disinfection strategies. In this study, we studied the 48 h kinetics of *Bacillus cereus* and *Escherichia coli* cells exposed to sub-MIC concentrations of didecyldimethylammonium chloride (DDAC). Two mathematical models were employed to reproduce the experiments: the only-growth classical logistic model and a mechanistic model including growth and death dynamics. Although both models reproduce the lag, exponential and stationary phases, only the mechanistic model is able to reproduce the death phase and reveals the concentration dependence of the bactericidal/bacteriostatic activity of DDAC. This model could potentially be extended to study other antimicrobials and reproduce changes in optical density (OD) and colony-forming units (CFUs) with the same parameters and mechanisms of action.

Keywords: dynamic modeling, disinfection, didecyldimethylammonium chloride (DDAC), *B. cereus*, *E. coli*, bacteriostatic, bactericidal, sub-MIC concentration

OPEN ACCESS

Edited by:

Santi M. Mandal,
Indian Institute of Technology
Kharagpur, India

Reviewed by:

Fernando Perez Rodriguez,
University of Cordoba, Spain
Krzysztof Skowron,
Nicolaus Copernicus University in
Toruń, Poland

*Correspondence:

José A. Vázquez
jvazquez@iim.csic.es
Miriam R. García
miriamr@iim.csic.es

Specialty section:

This article was submitted to
Antimicrobials, Resistance and
Chemotherapy,
a section of the journal
Frontiers in Microbiology

Received: 13 August 2021

Accepted: 09 February 2022

Published: 07 April 2022

Citation:

Pedreira A, Vázquez JA and
García MR (2022) Kinetics of Bacterial
Adaptation, Growth, and Death at
Didecyldimethylammonium Chloride
sub-MIC Concentrations.
Front. Microbiol. 13:758237.
doi: 10.3389/fmicb.2022.758237

1. INTRODUCTION

Designing effective disinfection strategies relies on understanding the mechanism of action (bacteriostatic, bactericidal, or both) and at which concentrations, using the well described and standardized minimum bactericidal concentration (MBC), minimum inhibitory concentration (MIC), or even others such as the non-inhibitory concentration (NIC) (Lambert and Pearson, 2000; EN-1276, 2009; ISO-20776-1, 2019).

Standard indexes of effective disinfectant concentrations are, however, endpoint static values, usually measured after 18 or 24 h of incubation and starting from a fixed inoculum without considering the inoculum effect and disregarding the bacterial kinetics (Mouton and Vinks, 2005; García and Cabo, 2018). Note that, even when effective supra-MBC treatments are applied, the kinetics of time-kill curves change with the disinfectant dose, as it has been widely analyzed in the literature using mathematical models (Gyrk and Finch, 1998; Peleg, 2021).

On the other hand, understanding the kinetics of ineffective disinfection treatments is also critical to prevent the emergence of resistance in bacteria. The non-volatile disinfectant may end

on the environment at sub-MIC concentrations (Holah et al., 2002; García and Cabo, 2018; Ribič et al., 2020) with the corresponding emergence of resistant strains to the used disinfectant or even other antimicrobials as antibiotics (Capita and Alonso-Calleja, 2013; Nordholt et al., 2021), being nowadays especially relevant due to the overuse of disinfectants during the current SARS-CoV-2 pandemic (Pedreira et al., 2021). Moreover, even when supra-MIC treatments are applied, growth may be observed due to many practical problems as interfering substances or bacterial formation of biofilms (Simões et al., 2010; Araújo et al., 2013).

Mathematical models analyzing the sub-MIC treatments, nevertheless, are only focused on non-disinfectant antimicrobials such as antibiotics or toxic substances or particles (Liu et al., 2005; Vázquez et al., 2011; Theophel et al., 2014) and are only-growth models disregarding any decrease in bacterial population numbers (Chatterjee et al., 2015). Models combining net growth and death rates are needed since sub-MIC kinetics curves show lag, exponential, stationary, and death phases and those models can help to determine if a disinfectant works by increasing the lag phase, decreasing the growth rate (bacteriostatic), increasing the death rate (bactericidal), or a combination of both mechanisms depending on its concentration.

The main urge to model sub-MIC kinetics is for quaternary ammonium compounds (QACs), non-volatile disinfectants with the risk to promote resistance (Kampf, 2018a). They are cost-effective disinfectants with detergency properties, and thus, they can be used as single-stage cleaning and disinfection agents in low soiling conditions. QACs are widely employed in industry, household and even cosmetics products as detergents, emulsifiers, softeners, disinfectants, or floating agents (Zhang et al., 2015). This family comprises several amphiphilic cationic surfactants with a general structure of $N+R_1R_2R_3R_4X^-$, where R represents a hydrogen atom, an alkyl group, or other functional groups, and X represents an anion (Buffet-Bataillon et al., 2012).

Didecyltrimethylammonium chloride (DDAC) is a commonly employed QAC formed by two alkyl chains each comprising of 10 (C10, didecyl) carbon atoms. UE legislation also includes under the name of DDAC such mixtures comprising C8 (octyl), C10, and C12 (dodecyl) chains, with at least 90% of C10 chains (EURL-SRM, 2016). DDAC is commonly found in the formulation of healthcare products and household cleaners/sanitizers as well as in the disinfection of surfaces and equipment in the food and feed areas both alone and in mixtures with other detergents (Lim and Chung, 2014; EURL-SRM, 2016). DDAC is especially common in the dairy industry, where it is widely used for disinfection of all kinds of surfaces on milking equipment, milk storage tanks, and machines and even in the disinfection of udders in order to prevent mastitis (EURL-SRM, 2016). When employed correctly, DDAC is considered safe to operatives and consumers and causes minimal corrosion of common materials, particularly compared to oxidative disinfectants.

Didecyltrimethylammonium chloride is antimicrobial acting on the bacterial membranes and showing bacteriostatic and bactericide activity depending on its concentration and the growth phase of the population (Yoshimatsu and Hiyama, 2007; Kampf, 2018a). The MIC values for DDAC vary among species

and isolates but its application at the recommended dosage in commercial disinfectants seems to be not always enough to inactivate all types of pathogens (Ramzi et al., 2020). In general, most bacteria isolated from food have MIC values ranging from 0.5 to 6.0 mg L⁻¹ (Kampf, 2018a). However, MIC values up to 1,024 mg L⁻¹ for DDAC and others QACs have been reported in bacteria isolated from retail meats in China (Zhang et al., 2016) and the USA (Zou et al., 2014).

Large DDAC MIC values could be related to the ability of bacteria to acquire resistance when exposed to sub-MIC concentrations, as have been observed in *Escherichia coli*, with an increase of 1.5 to 3-fold in MIC value (Kampf, 2018a). Moreover, DDAC could promote cross-resistance to other disinfectants and antibiotics (Langsrud et al., 2003; Walsh et al., 2003; Soumet et al., 2016; Kampf, 2018b). The presence of these sub-MIC disinfectant concentrations on surfaces can be explained as a consequence of an incorrect calculation of the disinfectant work concentration, the employ of expired or inappropriate stored substances (with the consequent decrease in efficiency), the lack of a successful pre-disinfection cleaning to remove organic matter (responsible of inactivation of disinfectant substances) or an irregular spreading (Capita et al., 2019).

The aim of this study is to motivate the need for new mechanistic models to study disinfection at sub-MIC treatments and demonstrate the insight gained by this analysis. The case study is the evaluation of the effect of DDAC on the growth of the common foodborne pathogens *E. coli* and *Bacillus cereus* (LeeNari et al., 2014) using measurements of optical density (OD) and colony-forming units (CFUs/ml). Two models are compared, the classical logistic only-growth model, where the DDAC effect is described using the Weibull functions, and a new mechanistic model that describes explicitly the mechanisms of adaptation, growth, and death using the Hill equations for the disinfectant effect. The mechanistic model shows a better goodness-of-fit for OD growth and is analyzed and extended to reproduce growth with both usual measurements (OD and CFUs/ml) and to understand DDAC treatment.

2. MATERIALS AND METHODS

2.1. Bacterial Strains and Culture Conditions

Nonpathogenic surrogate strains of *B. cereus* (CECT 495) and *E. coli* (CECT 102) were purchased to Colección Española de Cultivos Tipo (CECT, Universidad de Valencia, Spain). Both *B. cereus* and *E. coli* are common foodborne pathogens and were chosen by their differences at cell wall level, respectively Gram-positive and Gram-negative. Stock cultures were kept at -80°C in culture media supplemented with 25% (v/v) glycerol.

The culture media selected for the dose-response assays was meat-peptone broth (MPB) containing 5 g L⁻¹ meat extract (Scharlau SL, Barcelona, Spain), 10 g L⁻¹ neopeptone (Bacto™. BD Biosciences, Franklin Lakes, NJ, USA), and 5 g L⁻¹ NaCl (Emsure®, Merck KGaA, Darmstadt, Germany) in distilled water. DDAC (98 % purity; ABCR GmbH & Co KG, Karlsruhe, Germany) was added to the media to obtain the different

desired concentrations for sub-MIC treatments. The pH was adjusted to 7.2 and the media was finally sterilized by autoclaving (121°C/15 min). Dose-response assays were performed in 300 mL Erlenmeyer flasks containing 180 mL of MPB. Flasks were inoculated with 900 μL from a 21 h culture and incubated in an orbital shaker (200 rpm) at 30°C (*B. cereus*) or 37°C (*E. coli*). A previous screening was carried out to know the range of DDAC concentrations with partial inhibitory effect under our specific experimental conditions. The resulting DDAC concentrations selected were 0.5, 0.75, 1.00, 1.50, 2.00, and 3.00 mg L⁻¹ for *E. coli* and 0.05, 0.07, 0.25, 0.80, 1.00, and 1.50 mg L⁻¹ for *B. cereus*. Each DDAC concentration was tested by duplicate. At predetermined incubation times (0, 2, 4, 8, 12, 16, 20, 24, 30, 36, and 48 h), samples from each flask were taken and properly diluted in peptone-buffered water for OD determination at 700 nm. For comparative purposes, 1 mL samples from each flask were several-fold diluted in peptone-buffered solution and 0.1 mL aliquots were plated by duplicate on agarized MPB (2% w/v agar), resulting in a total of four plates per DDAC concentration tested for each strain. Plates were incubated at previously indicated temperatures for each strain and manually counted after 24–48 h of incubation.

2.2. Mathematical Modeling of Bacterial Dynamics at sub-MIC Concentrations

Different types of models have been studied in this study. First, we compared the performance of two types of models to reproduce OD growth and inhibition by DDAC: the classical logistic model with disinfectant inhibition following the Weibull functions and a dynamic model based on mechanisms of adaptation, growth, inhibition, and death. Second, we extend the mechanistic model to account for CFUs growth. Finally, we present the numerical methods used for the simulation, parameter estimation, and model analysis.

2.2.1. The Logistic Model With the Weibull Functions to Describe the Disinfectant Inhibition

The first model applied for the description of DDAC effect on bacterial growth measured with OD was a bivariate equation based on the combination of the Weibull function as biocide-concentration model modifying the most relevant kinetic-parameters of the reparametrized logistic equation used for the bacterial growth description (Rial et al., 2011; Vázquez et al., 2011):

$$OD = X = \frac{X_m}{1 + \exp\left(2 + \frac{4V_m}{X_m}(\lambda - t)\right)} \quad (1)$$

being X , the OD (absorbance at 700 nm, OD700) dependent on three functions of DDAC concentration (C) describing the maximum OD (X_m), the maximum growth rate (V_m), and the lag phase (λ). These functions are assumed that comply with the Weibull functions as follows:

$$X_m = X_m^0 \left[1 - K_x \left(1 - \exp \left\{ -\ln(2) \left(\frac{C}{m_x} \right)^{a_x} \right\} \right) \right] \quad (2)$$

TABLE 1 | Variables and parameters used for the logistic model.

Variables		Units
t	Time	h
X	Bacterial concentration measured with absorbance at 700 nm.	AU
X_m	Maximum bacterial load	AU
V_m	Maximum growth rate	AU h ⁻¹
λ	Lag phase	h
C	Concentration of disinfectant	mg L ⁻¹
Parameters		
X_m^0	Maximum bacterial load without disinfectant	AU
K_x	Maximum response affecting on X_m	1
m_x	Disinfectant corresponding to the semi-maximum response affecting on X_m	mg L ⁻¹
a_x	Shape parameter affecting on X_m	1
V_m^0	Maximum growth rate without disinfectant	AU h ⁻¹
K_v	Maximum response affecting on V_m	1
m_v	Disinfectant corresponding to the semi-maximum response affecting on V_m	mg L ⁻¹
a_v	Shape parameter affecting on V_m	1
λ^0	Lag phase without disinfectant	h
K_λ	Maximum response affecting on λ	1
m_λ	Disinfectant corresponding to the semi-maximum response affecting on λ	mg L ⁻¹
a_λ	Shape parameter affecting on λ	1

AU, Absorbance units.

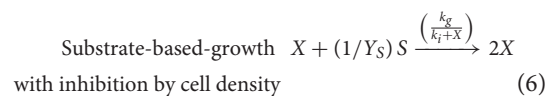
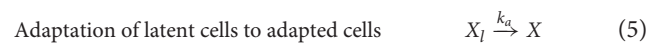
$$V_m = V_m^0 \left[1 - K_v \left(1 - \exp \left\{ -\ln(2) \left(\frac{C}{m_v} \right)^{a_v} \right\} \right) \right] \quad (3)$$

$$\lambda = \lambda^0 \left[1 - K_\lambda \left(1 - \exp \left\{ -\ln(2) \left(\frac{C}{m_\lambda} \right)^{a_\lambda} \right\} \right) \right] \quad (4)$$

Parameters meaning and units are summarized in **Table 1**.

2.2.2. The Mechanistic Model With the Hill Equations to Describe the Disinfectant Effect

As an alternative to the classical logistic model with the Weibull functions, we derived a model based on cell adaptation, substrate-based growth with inhibition by cell density and death. The idea can be outlined using the following biochemical reactions:



where X_I and X are, respectively, the OD of latent and adapted cells and S is the available substrate that is consumed (with yield coefficient Y) when adapted cells divide. The mass action was

assumed for all the biochemical reactions (i.e., constant rates, k_a and k_d for adaptation and death, respectively, multiplied for the reactants) with exception of the growth rate. In this reaction, we included the inhibition by cell density using Michaelis-Menten kinetics.

The mass balance of the reactions results on the following equations:

$$\frac{dX_l}{dt} = -k_a X_l - k_d X_l \quad (9)$$

$$\frac{dX}{dt} = k_a X_l + \left(\frac{k_g}{k_i + X} \right) SX - k_d X \quad (10)$$

$$\frac{dS}{dt} = -Y_S \left(\frac{k_g}{k_i + X} \right) SX \quad (11)$$

$$OD = (X_l + X) + \alpha X_d \quad (12)$$

$$CFUs = \beta 10^{10} (X_l + X) \quad (13)$$

consisting of three ordinary differential equations (ODEs) and two types of measurable variables:

- **Optical density:** sum of the contribution of the latent (X_l) and adapted cells (X) plus non-lysed death cells as assumed by Haque et al. (2017). Note that dead cells can be calculated as $X_d = X_l(t=0) - (X_l + X)$ and that the percentage of non-lysed cells is assumed constant and represented by $\alpha \in [0, 1]$.
- **Colony-forming units:** sum of alive cells (latent or adapted) multiplied by a scale factor.

To understand the effect of the disinfectant on the different mechanisms, we added dependence of the disinfectant concentration using the Hill equations:

$$k_g = k_g^0 \frac{IC_{50,g}^{\gamma_g}}{C^{\gamma_g} + IC_{50,g}^{\gamma_g}} \quad (14)$$

$$k_a = k_a^0 \frac{IC_{50,a}^{\gamma_a}}{C^{\gamma_a} + IC_{50,a}^{\gamma_a}} \quad (15)$$

$$k_d = k_d^0 + k_d^* \frac{C^{\gamma_d}}{C^{\gamma_d} + EC_{50,d}^{\gamma_d}} \quad (16)$$

where decreasing Hill functions are assumed to model inhibition of growth and adaptation rates with increasing disinfectant concentration (decreasing dose-response curves), and an increasing Hill function is assumed to describe the increase of the death rate with the disinfectant (increasing dose-response curve) (Mouton and Vinks, 2005; Santillán, 2008). In these equations, γ is the Hill coefficient shaping the effect of the disinfectant (higher values model sharp functions, similar to step functions with only two possible values, and low values describe an almost constant function except for a jump at zero and around 1 simulates a sigmoid curve) and IC_{50} and EC_{50} are the half maximal inhibitory/effective concentration (disinfectant concentrations at which 50% of the maximum effect is obtained). Note that without disinfectant the growth and adaptation velocities correspond with k_g^0 and k_a^0 . In absence of disinfectant, we allow death at k_d^0 to reproduce the final death phase, whereas k_d^* scales the effect of the disinfectant. The variables and parameters are summarized in **Table 2**.

TABLE 2 | Variables, initial conditions, and parameters used for the mechanistic model.

Variables		Units
t	Time	h
X_l	Optical density of latent cells	AU
X	Optical density of adapted cells	AU
S^\dagger	Substrate for growth (availability of resources)	1
C	Concentration of disinfectant	mg L ⁻¹
$K_a = k_a$	Adaptative specific rate	h ⁻¹
$K_g = \frac{k_g}{k_i + X}$	Growth specific rate	h ⁻¹
$K_d = k_d$	Death specific rate	h ⁻¹
Initial conditions		
$X_l(t=0) = OD(t=0)$	Initial density of latent cells	AU
$X(t=0) = 0$	Initial density of adapted cells	AU
$S(t=0) = 1$	Initial substrate density, normalized to 1	1
Parameters		
k_a^0	Adaptation rate without disinfectant	h ⁻¹
k_g^0	Growth rate without disinfectant	AU h ⁻¹
k_d^0	Death rate without disinfectant	h ⁻¹
k_d^*	Scaling of disinfectant effect on death	h ⁻¹
k_i	Inhibition constant due to cell density	AU
$IC_{50,a}$	Half maximal inhibitory concentration of adaptation rate	mg L ⁻¹
$IC_{50,g}$	Half maximal inhibitory concentration of growth rate	mg L ⁻¹
$EC_{50,d}$	Half maximal effective concentration on death	mg L ⁻¹
γ_a	Effect shape of disinfectant over adaptation rate	1
γ_g	Effect shape of disinfectant over growth rate	1
γ_d	Effect shape of disinfectant over death rate	1
Y_S	Yield coefficient	1/AU
α	Contribution of death cells to OD	1
β	Scaling factor from OD to CFUs	CFUs /AU mL

AU, Absorbance units. [†] Normalized substrate concentration is considered as the initial substrate is not identifiable.

2.3. Numerical Methods

For the model simulation, calibration (estimation of unknown parameters), and analysis, we use numerical methods implemented in AMIGO2 (Advanced Model Identification using Global Optimization) software, a multi-platform toolbox implemented in Matlab (Balsa-Canto et al., 2016b). The code, with all the selected options for simulation and optimization, is freely available at <https://doi.org/10.5281/zenodo.5167910>.

For the model calibration, we have selected the maximization of the log-likelihood function, equivalent under common assumptions [refer to Balsa-Canto et al. (2016a) for details] to minimize the least-squares function (squares of the residuals) divided by the standard deviation. In this study, we calculate the standard deviation for each time-point from the experimental replicates (refer to calculated standard deviations for each time-point in **Supplementary Figure S1** and calculate the mean for each bacteria (*B. cereus*, *E. coli*) and type of data (CFUs, OD).

Therefore, the objective is to find the parameters that minimize:

$$J = \frac{1}{\sigma^2} \sum_{j=1}^{n_{exp}} \sum_{i=1}^{n_t} (Y_{ij} - \hat{Y}_{ij})^2, \text{ with } \sigma = \overline{\sigma_{ij}} \quad (17)$$

where n_{exp} and n_t are the number of experiments (seven including the control without disinfectant for each bacterial strain) and the number of time data points, respectively, and being Y , σ , and \hat{Y} the data, standard deviation, and model predictions, respectively. Bounds considered for the parameters were $[0, 15]$ with the exception of $\alpha \in [0, 1]$ and $\beta \in [0, 100]$.

The confidence intervals for the parameters were estimated by $\pm t_{\alpha/2}^{\gamma} \sqrt{C_{ii}}$, where C_{ii} are the diagonal elements of the confidence matrix, $t_{\alpha/2}^{\gamma}$ is given by Student's t -distribution with γ the number of degrees of freedom and $(1 - \alpha)100\%$ selected to 95%. The Cramér-Rao inequality was employed to compute a bound for the confidence matrix using the Fisher information matrix (Balsacanto et al., 2016a).

To compare the performance among models, we employed the following well-known indexes: the adjusted R^2 , the

corrected Akaike information criterion (AICc), and the Bayesian information criterion (BIC). The three indexes are a function of the error existing between model and experimental data, penalizing the number of parameters to be estimated. Indexes with lower numbers imply better performance.

3. RESULTS AND DISCUSSION

3.1. Modeling Growth Measured With OD

In this study, we compared a classical model (logistic growth with inhibition using the Weibull functions) with a model derived from mechanisms (inspired by biochemical reactions of adaptation, substrate-based growth with inhibition by cell density and death).

As explained in section 2.2.1, the classical model describes the effect of DDAC on bacterial growth based on the combination of the Weibull function as biocide-concentration model modifying the most relevant kinetic-parameters of the reparametrized logistic equation used for the bacterial growth description. We should mention that the derivative form of this model was used

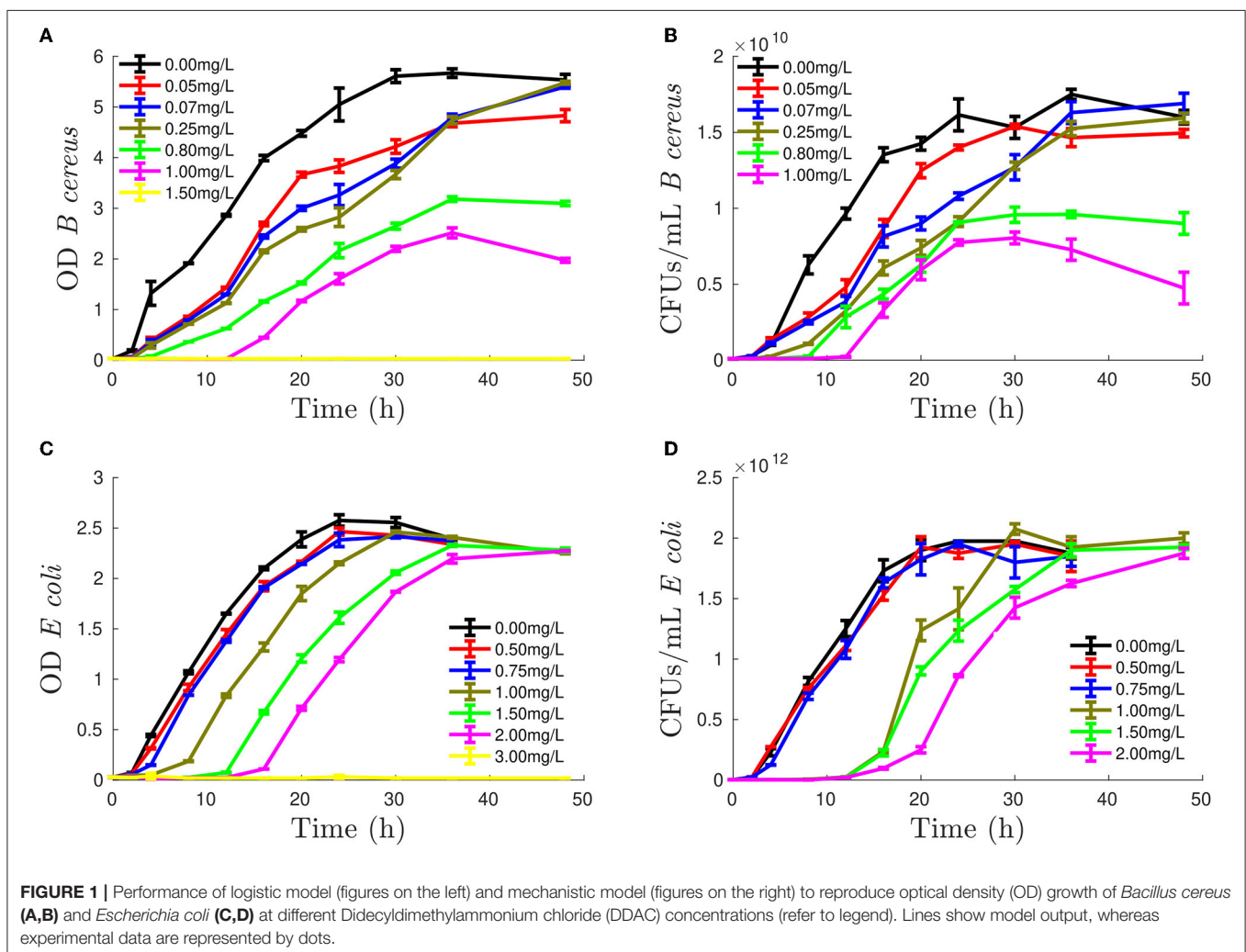
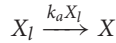


FIGURE 1 | Performance of logistic model (figures on the left) and mechanistic model (figures on the right) to reproduce optical density (OD) growth of *Bacillus cereus* (A,B) and *Escherichia coli* (C,D) at different Didecylidimethylammonium chloride (DDAC) concentrations (refer to legend). Lines show model output, whereas experimental data are represented by dots.

to allow its implementation in the AMIGO2 software, refer to <https://doi.org/10.5281/zenodo.5167910> for details.

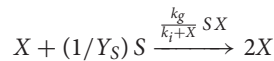
On the other hand, the model derived in this study assumes the following mechanisms (refer to section 2.2.2 for mathematical details of the model):

- Initially, cells are in a latent state (X_l) without the potential to divide. The adaptation of latent cells can be interpreted in terms of the following biochemical reaction:



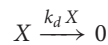
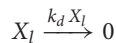
where the specific adaptation rate (or rate per capita) is a Hill-decreasing-function of the disinfectant concentration $k_a(C)$, as described later, and the total rate follows the mass action law ($K_a = k_a X$).

- Adapted cells (X) grow if there is disponibility of nutrients (substrate S) and this growth is inhibited by cell density using Michaelis–Menten kinetics. The biochemical representation is as follows:



where $1/Y_S$ is the yield coefficient, the specific growth rate is again a Hill-decreasing-function of disinfectant $k_g(C)$ and k_i is the coefficient regulating the inhibition due to cell density (with low values for strong inhibition by large cell numbers). Note that this inhibition encodes different mechanisms like the inhibition for the production of waste in a cell cycle. This biochemical reaction describes both the exponential growth phase and the stationary phase.

- Latent and adapted cells may die:



Death occurs with a specific rate dependent on a Hill-increasing function on the concentration of disinfectant $k_d(C)$. Note that death may be active during the whole dynamics and determines the death phase when this rate surpasses the growth rate (negative cell growth).

- Cellular adaptation, growth, and death are assumed to depend on DDAC concentration. As adaptation and growth rates commonly decrease with disinfectant concentration, we selected a decreasing dose-response curve, whereas for death an increasing dose-response curve was assumed. For the shape of the dose-response, we employed the Hill Equations (14–16): standard functions on pharmacodynamics selected due to their flexibility and their mechanistic interpretation, providing estimations of half maximal inhibitory/effective concentration of the disinfectant over the different mechanisms (Regoes et al., 2004).
- Optical density includes the direct contribution of the latent and adapted viable cells plus some contribution [to be estimated, as previously assumed in Haque et al. (2017)] of

TABLE 3 | Performance of both models to reproduce the data (measured in terms of the Adjusted R^2 , AICc, BIC) and estimated parameters.

	<i>B. cereus</i>		<i>E. coli</i>	
	Logistic model	Mechanistic model	Logistic model	Mechanistic model
Adj. R^2	0.97	0.98	0.99	1.00
AICc	3,116.59	1,831.19	16,229.24	7,152.58
BIC	3,141.37	1,857.59	16,253.38	7,178.28
Parameters	$X_m^0 = 5.3$ $K_x = 14$ $m_x = 6.9$ $a_x = 1.5$ $V_m^0 = 0.33$ $K_v = 1.1$ $m_v = 5$ $a_v = 0.11$ $\lambda^0 = 3.2$ $K_\lambda = 10$ $m_\lambda = 3.2$ $a_\lambda = 0.65$	$k_a^0 = 15$ $k_g^0 = 0.59$ $k_i^0 = 0.003$ $k_x^* = 15$ $k_j = 0.51$ $IC_{50,a} = 0.021$ $IC_{50,g} = 15$ $EC_{50,d} = 3.1$ $\gamma_a = 1.9$ $\gamma_g = 0.076$ $\gamma_d = 4.7$ $Y_S = 0.16$ $\alpha = 0.32$	$X_m^0 = 2.4$ $K_x = 11$ $m_x = 4.2$ $a_x = 6.2$ $V_m^0 = 0.19$ $K_v = 0.19$ $m_v = 0.91$ $a_v = 15$ $\lambda^0 = 3$ $K_\lambda = 4.7$ $m_\lambda = 1.3$ $a_\lambda = 2.9$	$k_a^0 = 0.35$ $k_g^0 = 0.33$ $k_i^0 = 0.023$ $k_x^* = 12$ $k_j = 0.24$ $IC_{50,a} = 0.71$ $IC_{50,g} = 15$ $EC_{50,d} = 3.7$ $\gamma_a = 15$ $\gamma_g = 0.68$ $\gamma_d = 14$ $Y_S = 0.22$ $\alpha = 0.0001$

the dead cells (including those viable but not cultivable cells undetected by plating). Mathematically, this is expressed as follows where dead cells can be calculated as the initial total cells [only latent cells $X_l(t = 0)$] minus latent and adapted cells at a given time:

$$OD = (X_l + X) + \alpha X_d = (X_l + X) + \alpha [X_l(t = 0) - (X_l + X)]$$

Under these assumptions, we derived a model consisting of a set of three ODEs plus an algebraic equation defining the measured variable OD (refer to section 2.2.2). We should mention that for its implementation in the AMIGO2 toolbox, the derivative equation of the OD function was implemented. Refer to code for details at <https://doi.org/10.5281/zenodo.5167910>.

Figure 1 depicts the performance of the logistic and mechanistic model to reproduce the growth of *B. cereus* and *E. coli* measured using OD. Both models reproduce the data trends, with the main difference being the ability of the mechanistic model to describe the smooth transition to the stationary phase in *B. cereus* (**Figure 1B**) and the initial death phase for *E. coli* (**Figure 1D**). Moreover, the mechanistic model starts from the experimental initial conditions, whereas the logistic model allows flexibility for this condition.

Table 3 shows three standard indexes to measure the model's ability to reproduce the data penalizing overparametrisation: the adjusted R^2 , the corrected AICc, and the BIC. All criteria show a lower value (despite penalizing the models with many degrees of freedom) for the mechanistic model, where 13 parameters were estimated instead of the 12 estimation parameters for the logistic model.

The mechanistic model was selected for the rest of the study due to a better goodness-of-fit and its mechanistic insight.

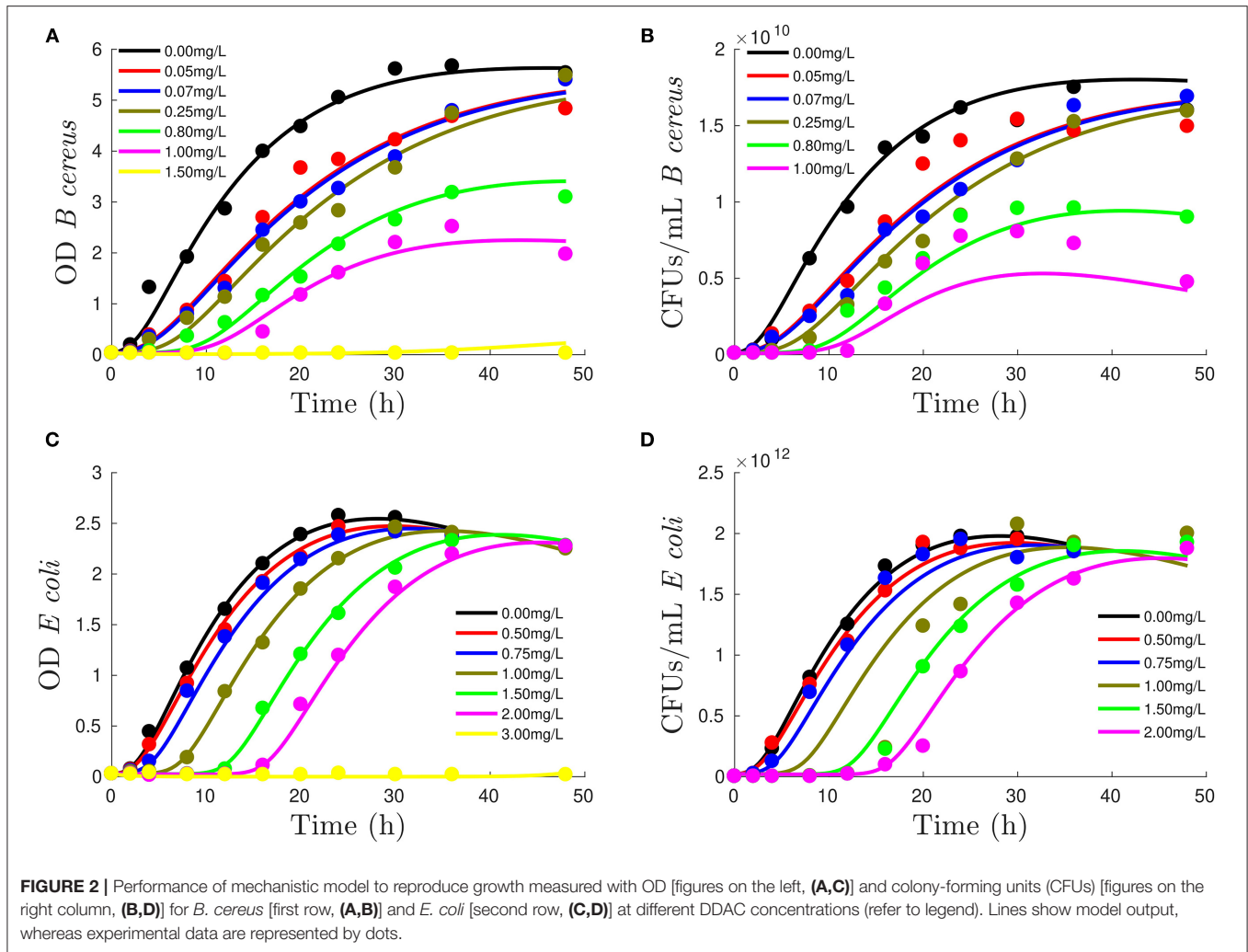


FIGURE 2 | Performance of mechanistic model to reproduce growth measured with OD [figures on the left, (A,C)] and colony-forming units (CFUs) [figures on the right column, (B,D)] for *B. cereus* [first row, (A,B)] and *E. coli* [second row, (C,D)] at different DDAC concentrations (refer to legend). Lines show model output, whereas experimental data are represented by dots.

We want to stress that although both models show good performance, which was only slightly lower for the classical model, the insight from the mechanistic model was determinant to make the decision. Mechanistic models allow a deeper study of the process and (as shown in the next section) can be extended to account also for CFUs by adding only one extra parameter.

3.2. Extending the Mechanistic Model to Reproduce Growth Measured With CFUs

Both OD and CFUs are related standard methods to measure bacterial concentration dynamics but differ in their interpretation. OD is a fast method but is affected by many factors, including dead cells in the medium with intact cell wall (Stevenson et al., 2016), making estimations of alive cells unreliable, whereas CFUs provides reliable estimations of viable cells, but it is experimentally time-consuming. Estimations using only CFUs were tested with both logistic and mechanistic models (data not shown), with better estimations for the mechanistic model for including the death phase observed in the data.

We extended the mechanistic model derived in this study to explain both, OD and CFUs data. Let us recall here the OD variable:

$$OD = (X_l + X) + \alpha X_d$$

being a function of latent, adapted, and dead cells. For the modeling of CFUs, we consider only alive cells (either latent or adapted):

$$CFUs = \beta 10^{10} (X_l + X)$$

with $\beta 10^{10}$ a scaling factor transforming OD to CFUs.

Figure 2 shows how assumed mechanisms are sufficient to reproduce OD and CFUs using the same adaptation, growth, and death parameters. The mechanistic model has 14 parameters: 12 common parameters plus α , defining contribution of dead cells to OD, and $\beta 10^{10}$, which represents the difference between OD (usually one order of magnitude) and CFUs (varying from 10 orders of magnitude for *B. cereus* and 12 for *E. coli*).

Table 4 shows the model performance in terms of adjusted R^2 , AICc, and BIC. Note that now the model has been

challenged to reproduce both OD and CFUs with the same parameters and, although indexes are acceptable for the measured experimental errors, are worse than when reproducing only OD. To further analyze that the performance is satisfactory, we have included the confidence intervals of the estimated parameters, where the data uncertainty is also considered (refer to **Supplementary Figure S1**).

The graphical picture of how adaptation, growth, and death-specific rates change with DDAC is shown in **Figure 3**. Note that growth-specific rate is inhibited by limiting substrates and large cell density. To simplify the figure, we plotted k_g assuming that resources are not limiting (S is almost constant) and inhibition by cell density is not relevant, and therefore, $K_g \approx k_g$.

TABLE 4 | Results (performance indexes and estimated parameters with their confidence intervals) for the extended mechanistic model to account for both OD and CFUs growth with DDAC.

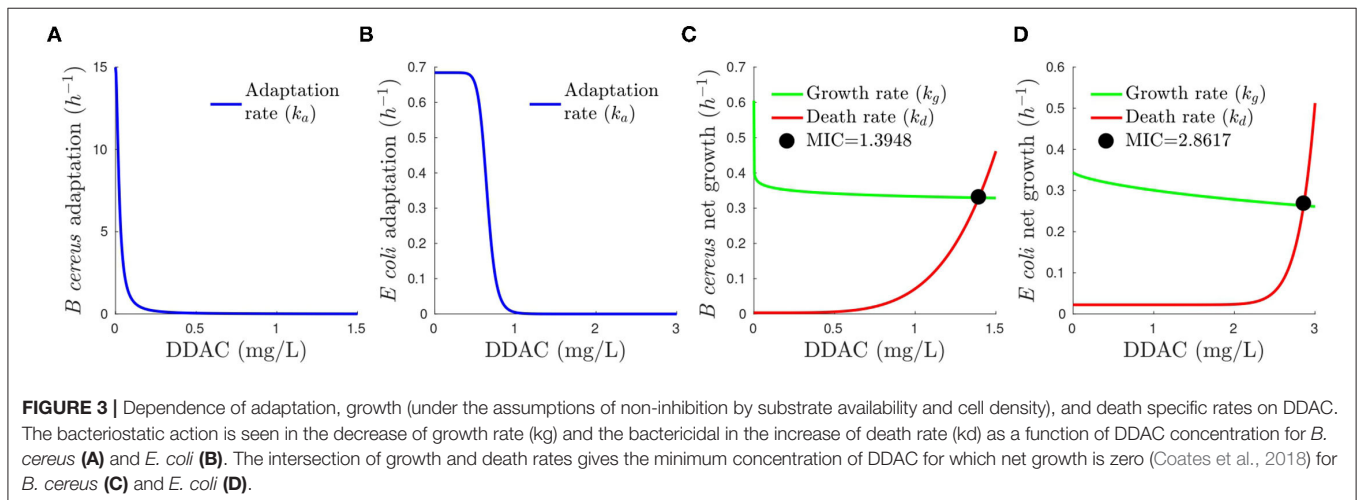
	<i>B. cereus</i>	<i>E. coli</i>
Adj. R ²	0.96	0.96
AICc	3,147.29	21,026.27
BIC	3,188.28	21,066.64
Parameters ± CI		
	$k_a^0 = 15 \pm 63$	$k_a^0 = 0.68 \pm 0.13$
	$k_g^0 = 0.6 \pm 0.025$	$k_g^0 = 0.34 \pm 0.0059$
	$k_d^0 = 0.0035 \pm 0.0016$	$k_d^0 = 0.022 \pm 0.0015$
	$k_g^* = 13 \pm 62$	$k_g^* = 15 \pm 2.2$
	$k_i = 0.54 \pm 0.057$	$k_i = 0.29 \pm 0.016$
	$IC_{50,a} = 0.023 \pm 0.053$	$IC_{50,a} = 0.65 \pm 0.0068$
	$IC_{50,g} = 14 \pm 24$	$IC_{50,g} = 15 \pm 2.2$
	$EC_{50,d} = 3 \pm 3.3$	$EC_{50,d} = 3.8 \pm 0.05$
	$\gamma_a = 1.8 \pm 0.22$	$\gamma_a = 12 \pm 0.46$
	$\gamma_g = 0.078 \pm 0.024$	$\gamma_g = 0.71 \pm 0.039$
	$\gamma_d = 4.8 \pm 0.25$	$\gamma_d = 15 \pm 0.61$
	$Y_S = 0.16 \pm 0.0067$	$Y_S = 0.23 \pm 0.0082$
	$\alpha = 0.28 \pm 0.027$	$\alpha = 6.9e-07 \pm 0.013$
	$\beta = 0.33 \pm 0.0045$	$\beta = 78 \pm 0.47$

3.3. Discussion

In this study, we derived a new mechanistic model able to represent the different phases (adaptation, growth, stationary, and death) at sub-MIC concentrations of DDAC. The logistic model, the standard model used to quantify growth inhibition with bacteriostatic antimicrobials, was unable to reproduce the last death phase of the growth curves. This limitation was previously detected when modeling the inhibition of *E. coli* and *Staphylococcus aureus* due to silver nanoparticles (Chatterjee et al., 2015). As with sub-MIC DDAC concentrations, nanoparticles are mostly bacteriostatic but growth curves show a decline at long times.

The derived model was calibrated from and did reproduce the two most common measurements of bacterial population numbers, OD and CFUs, using the same parameters for adaptation, growth, and death rate. Results show that *E. coli* dead cells do not affect OD, probably due to severe cell lysis and their not appreciable effect in OD measurement (Stevenson et al., 2016). However, 32% of *B. cereus* dead cells contribute to OD. Two hypotheses can explain this estimation: either this contribution is due to viable but nonculturable cells or either some cells are non-lysed since *B. cereus* has more resistance to lysis than *E. coli* (Fykse et al., 2003).

The analysis of the developed model confirms the literature observation that DDAC is bacteriostatic and bactericidal depending on its concentration and the growth phase of the microbial population (Yoshimatsu and Hiyama, 2007; Kampf, 2018a). The growth rate is affected in both *B. cereus* and *E. coli*. In *B. cereus* the growth decreases sharply only by adding low concentrations of DDAC and remains almost constant afterward (γ_g close to zero), as can be seen in **Figure 3**, being, therefore, $IC_{50,g}$ irrelevant and with large uncertainty. Although Hill functions are very uncertain, and not useful to infer exactly at which concentration is this sharp decrease, the growth rate should be at least 0.6 h^{-1} when DDAC = 0 mg L^{-1} and 0.4 h^{-1} for DDAC = 0.5 mg L^{-1} (the DDAC concentrations experimentally tested) to fit the data. In *E. coli*, growth decreases smoothly when DDAC increases ($\gamma_g = 0.078$ and $IC_{50,g} = 14$). This can be also observed in **Figures 3C,D** for *B. cereus* and *E. coli*, respectively.



On the other hand, the bactericidal effect is also detected for both *B. cereus* and *E. coli* despite being the estimated dying rates the most uncertain model kinetics (as evidenced by the parameter confidence intervals). Whereas for *B. cereus* the bactericidal effect increases smoothly with DDAC concentration (**Figure 3C**), this behavior is more abrupt for *E. coli*.

The model also allows the study of the DDAC changes in the lag phase, a mechanism that is not considered when simply classifying a disinfectant as bacteriostatic or bactericidal. Adaptation is fast in *B. cereus* (small lag phase) and slow in *E. coli*. The model captures this behavior using larger values of k_a for *B. cereus* (maximum allowed value $k_a^0 = 15$) than for *E. coli* ($k_a^0 = 0.35$). Note that large confidence intervals are reported for *B. cereus* adaptation rate as faster adaptation rates result in the same dynamics where adaptation is complete within minutes or seconds at $c = 0$. Despite both strains showing the different magnitude of adaptation, the change of adaptation with DDAC concentration (**Figures 3A,B**) shows a similar trend. Whereas for both adaptation is high without DDAC, when DDAC concentration increases there is a deep decrease of adaptation, therefore, showing longer lag phases at high DDAC concentrations.

The analysis of the lag phase with DDAC concentration is particularly relevant to understanding the implications of MIC values and how they depend on the growth phase (Yoshimatsu and Hiyama, 2007; Kampf, 2018a). Lack of growth after 24 h could be due to different mechanisms: either an extremely large lag phase or that the death rate is equal or larger than the growth rate [zero or negative net growth rate, also commented by Mouton and Vinks (2005) the stationary concentration]. Assuming no effect of the limiting substrate and MIC representing the concentration of zero growth rate (Coates et al., 2018), the model can be used to calculate the MIC using the intersection of growth and death rate (k_g and k_d). As shown in **Figure 3C** there is net growth of *B. cereus* for disinfectant concentrations below 1.39 mg/L and the bacteriostatic effect is greater at low concentrations of DDAC whereas the bactericidal effect is higher at larger concentrations. On the other hand **Figure 3D** shows a similar trend, but with less bacteriostatic effect and with a MIC of 2.86 mg/L.

4. CONCLUSION

A new mathematical model capable to reproduce net growth and death kinetics is derived to study DDAC effects at sub-MIC concentrations. The model describes DDAC influence on adaptation, growth, stationary, and death phases and discerns if the disinfectant is bactericidal, bacteriostatic, or both, and at which concentrations. The model also considers adaptation, which is relevant to detect if the absence of growth after treatment is due to the use of supra-MIC treatments or because there is a

strong delay in the lag phase and bacteria can grow hours later, as observed in *E. coli* experiments. The analysis of the model reveals that DDAC is both bacteriostatic and bactericidal but mainly bacteriostatic at low sub-MIC concentrations and bactericidal at large sub-MIC concentrations.

Moreover, the model is able to reproduce the behavior of both OD and CFUs measurements using the same mechanisms and it is sufficiently flexible to account for different forms of the disinfectant effect and could be used to study the mechanisms of action of different types of antimicrobials, like antibiotics, at sub-MIC concentrations.

DATA AVAILABILITY STATEMENT

The datasets and mathematical models presented in this study can be found online in the following public repository <https://doi.org/10.5281/zenodo.5167910>.

AUTHOR CONTRIBUTIONS

AP and JAV designed the experimental study, conducted the experiments, and analyzed the data. AP and MG designed the theoretical study and conducted the computational experiments and analysis. All the authors drafted the manuscript and approved the final version.

FUNDING

This study was funded by the projects RTI2018-093560-J-I00 (MCIU/AEI/FEDER, UE), RYC2019-028006-I/AEI/10.13039/501100011033, 20213AT001, and the Xunta de Galicia Grants IN606A-2020/028 and IN607B-2021/11.

ACKNOWLEDGMENTS

We really thank Ana Isabel Durán and Araceli Mendiña for their great technical support during bacterial growth experiments.

SUPPLEMENTARY MATERIAL

The Supplementary Material for this article can be found online at: <https://www.frontiersin.org/articles/10.3389/fmicb.2022.758237/full#supplementary-material>

Figure S1 | Experimental data showing OD and CFUs growth of *B. cereus* (**A,B**) and OD and CFUs growth of *E. coli* (**C,D**) at different concentrations of DDAC. Standard deviation (error bars) and mean value (center of error bars) are represented. Shows experimental data means and variability for *B. cereus* and *E. coli*. Model files, experimental data, and scripts to reproduce results can be found in the following public repository <https://doi.org/10.5281/zenodo.5167910>.

REFERENCES

- Araújo, P. A., Lemos, M., Mergulhão, F., Melo, L., and Simões, M. (2013). The influence of interfering substances on the antimicrobial activity of selected quaternary ammonium compounds. *Int. J. Food Sci.* 2013, 237581. doi: 10.1155/2013/237581
- Balsa-Canto, E., Alonso, A., Arias-Méndez, A., García, M., López-Núñez, A., Mosquera-Fernández, M., et al. (2016a). *Modeling and Optimization Techniques With Applications in Food Processes, Bio-Processes and Bio-Systems*, Vol. 9. Springer. Available online at: https://link.springer.com/chapter/10.1007/978-3-319-32146-2_4
- Balsa-Canto, E., Henriques, D., Gábor, A., and Banga, J. R. (2016b). AMIGO2, a toolbox for dynamic modeling, optimization and control in systems biology. *Bioinformatics* 32, 3357–3359. doi: 10.1093/bioinformatics/btw411
- Buffet-Bataillon, S., Tattevin, P., Bonnaure-Mallet, M., and Jolivet-Gougeon, A. (2012). Emergence of resistance to antibacterial agents: the role of quaternary ammonium compounds - a critical review. *Int. J. Antimicrob. Agents* 39, 381–389. doi: 10.1016/j.ijantimicag.2012.01.011
- Capita, R., and Alonso-Calleja, C. (2013). Antibiotic-resistant bacteria: a challenge for the food industry. *Crit. Rev. Food Sci. Nutr.* 53, 11–48. doi: 10.1080/10408398.2010.519837
- Capita, R., Vicente-Velasco, M., Rodríguez-Melcón, C., García-Fernández, C., Carballo, J., and Alonso-Calleja, C. (2019). Effect of low doses of biocides on the antimicrobial resistance and the biofilms of *Cronobacter sakazakii* and *Yersinia enterocolitica*. *Sci. Rep.* 9, 1–12. doi: 10.1038/s41598-019-51907-1
- Chatterjee, T., Chatterjee, B. K., Majumdar, D., and Chakrabarti, P. (2015). Antibacterial effect of silver nanoparticles and the modeling of bacterial growth kinetics using a modified gompertz model. *Biochimica et Biophysica Acta (BBA)-General Subjects* 1850, 299–306. doi: 10.1016/j.bbagen.2014.10.022
- Coates, J., Park, B. R., Le, D., Şimşek, E., Chaudhry, W., and Kim, M. (2018). Antibiotic-induced population fluctuations and stochastic clearance of bacteria. *eLife* 7, 1–26. doi: 10.7554/eLife.32976
- EN-1276. (2009). *Chemical disinfectants and antiseptics in: Quantitative suspension test for the evaluation of bactericidal activity of chemical disinfectants and antiseptics used in food, industrial, domestic, and institutional areas - Test method and requirements (phase 2, step 1)*. European Standard EN-1276, 2009. Available online at: <https://standards.iteh.ai/catalog/standards/cen/d7ba84f4-a83b-46a7-8065-c638f57a9111/en-1276-2009>
- EURL-SRM (2016). Analysis of quaternary ammonium compounds (QACs) in fruits and vegetables using QuEChERS and LC-MS/MS. *EU Ref. Lab. Residues Pesticides Single Residue Methods* 5, 1–6. Available online at: https://www.eurl-pesticides.eu/userfiles/file/EurlSRM/EurlSRM_meth_QAC_ShortMethod.pdf
- Fykse, E. M., Olsen, J. S., and Skogan, G. (2003). Application of sonication to release dna from bacillus cereus for quantitative detection by real-time pcr. *J. Microbiol. Methods* 55, 1–10. doi: 10.1016/S0167-7012(03)00091-5
- García, M. R., and Cabo, M. L. (2018). Optimization of *E. coli* inactivation by benzalkonium chloride reveals the importance of quantifying the inoculum effect on chemical disinfection. *Front. Microbiol.* 9, 1259. doi: 10.3389/fmicb.2018.01259
- Gyrk, L. L., and Finch, G. R. (1998). Modeling water treatment chemical disinfection kinetics. *J. Environ. Eng.* 124, 783–793.
- Haque, M. A., Imamura, R., Brown, G. A., Krishnamurthi, V. R., Niyonshuti, I. I., Marcelle, T., et al. (2017). An experiment-based model quantifying antimicrobial activity of silver nanoparticles on: *Escherichia coli*. *RSC Adv.* 7, 56173–56182. doi: 10.1039/C7RA10495B
- Holah, J., Taylor, J., Dawson, D., and Hall, K. (2002). Biocide use in the food industry and the disinfectant resistance of persistent strains of *Listeria monocytogenes* and *Escherichia coli*. *J. Appl. Microbiol.* 92, 111S–120S. doi: 10.1046/j.1365-2672.92.5s1.18.x
- ISO-20776-1. (2019). *Susceptibility testing of infectious agents and evaluation of performance of antimicrobial susceptibility test devices - Part 1: Broth micro-dilution reference method for testing the in vitro activity of antimicrobial agents against rapidly growing aerobic bacteria involved in infectious diseases*. ISO 20776-1, 2019. Available online at: <https://www.iso.org/standard/70464.html>
- Kampf, G. (2018a). *Antiseptic Stewardship*. Springer. Available online at: <https://link.springer.com/content/pdf/10.1007/978-3-319-98785-9.pdf>
- Kampf, G. (2018b). Biocidal agents used for disinfection can enhance antibiotic resistance in gram-negative species. *Antibiotics* 7, 110. doi: 10.3390/antibiotics7040110
- Lambert, R. J., and Pearson, J. (2000). Susceptibility testing: accurate and reproducible minimum inhibitory concentration (MIC) and non-inhibitory concentration (NIC) values. *J. Appl. Microbiol.* 88, 784–790. doi: 10.1046/j.1365-2672.2000.01017.x
- Langsrud, S., Sundheim, G., and Borgmann-Strahsen, R. (2003). Intrinsic and acquired resistance to quaternary ammonium compounds in food-related *Pseudomonas* spp. *J. Appl. Microbiol.* 95, 874–882. doi: 10.1046/j.1365-2672.2003.02064.x
- LeeNari, Yoon, K., Kyung, O., ChangHyun-Joo, Sook, C., and ChoiSung-Wook (2014). A Multiplex PCR assay for simultaneous detection of *Escherichia coli* O157:H7, *Bacillus cereus*, *Vibrio parahaemolyticus*, *Salmonella* spp., *Listeria monocytogenes*, and *Staphylococcus aureus* in Korean ready-to-eat food. *Foodborne Pathog. Dis.* 11, 574–580. doi: 10.1089/fpd.2013.1638
- Lim, C. H., and Chung, Y. H. (2014). Effects of didecyldimethylammonium chloride on sprague-dawley rats after two weeks of inhalation exposure. *Toxicol. Res.* 30, 205–210. doi: 10.5487/TR.2014.30.3.205
- Liu, P., Rand, K. H., Obermann, B., and Derendorf, H. (2005). Pharmacokinetic-pharmacodynamic modelling of antibacterial activity of cefepodoxime and cefixime in in vitro kinetic models. *Int. J. Antimicrob. Agents* 25, 120–129. doi: 10.1016/j.ijantimicag.2004.09.012
- Mouton, J. W., and Vinks, A. A. (2005). Pharmacokinetic/pharmacodynamic modelling of antibacterials in vitro and in vivo using bacterial growth and kill kinetics the minimum inhibitory concentration versus stationary concentration. *Clin. Pharmacokinet.* 44, 201–210. doi: 10.2165/00003088-200544020-00005
- Nordholt, N., Kanaris, O., Schmidt, S. B., and Schreiber, F. (2021). Persistence against benzalkonium chloride promotes rapid evolution of tolerance during periodic disinfection. *Nat. Commun.* 12, 1–13. doi: 10.1038/s41467-021-27019-8
- Pedreira, A., Taşkın, Y., and García, M. R. (2021). A critical review of disinfection processes to control SARS-CoV-2 transmission in the food industry. *Foods* 10, 283. doi: 10.3390/foods10020283
- Peleg, M. (2021). Modeling the dynamic kinetics of microbial disinfection with dissipating chemical agents—a theoretical investigation. *Appl. Microbiol. Biotechnol.* 105, 539–549. doi: 10.1007/s00253-020-11042-8
- Ramzi, A., Oumokhtar, B., Ez Zoubi, Y., Filali Mouattassem, T., Benboubker, M., and El Ouali Lalami, A. (2020). Evaluation of antibacterial activity of three quaternary ammonium disinfectants on different germs isolated from the hospital environment. *BioMed Res. Int.* 2020, 6509740. doi: 10.1155/2020/6509740
- Regoes, R. R., Wiuff, C., Zappala, R. M., Garner, K. N., Baquero, F., and Levin, B. R. (2004). Pharmacodynamic functions: a multiparameter approach to the design of antibiotic treatment regimens. *Antimicrob. Agents Chemother.* 48, 3670. doi: 10.1128/AAC.48.10.3670-3676.2004
- Rial, D., Vázquez, J. A., and Murado, M. A. (2011). Effects of three heavy metals on the bacteria growth kinetics: a bivariate model for toxicological assessment. *Appl. Microbiol. Biotechnol.* 90, 1095–1109. doi: 10.1007/s00253-011-3138-1
- Ribič, U., Jakše, J., Toplak, N., Koren, S., Kovač, M., Klančnik, A., et al. (2020). Transporters and efflux pumps are the main mechanisms involved in *Staphylococcus epidermidis* adaptation and tolerance to didecyldimethylammonium chloride. *Microorganisms* 8, 344. doi: 10.3390/microorganisms8030344
- Santillán, M. (2008). On the use of the hill functions in mathematical models of gene regulatory networks. *Math. Model. Nat. Phenom* 3, 85–97. doi: 10.1051/mmnp:2008056
- Simões, M., Simões, L. C., and Vieira, M. J. (2010). A review of current and emergent biofilm control strategies. *LWT Food Sci. Technol.* 43, 573–583. doi: 10.1016/j.lwt.2009.12.008
- Soumet, C., Méheust, D., Pissavin, C., Le Grandois, P., Frémaux, B., Feurer, C., et al. (2016). Reduced susceptibilities to biocides and resistance to antibiotics

- in food-associated bacteria following exposure to quaternary ammonium compounds. *J. Appl. Microbiol.* 121, 1275–1281. doi: 10.1111/jam.13247
- Stevenson, K., McVey, A. F., Clark, I. B. N., Swain, P. S., and Pilizota, T. (2016). General calibration of microbial growth in microplate readers. *Sci. Rep.* 6, 1–7. doi: 10.1038/srep38828
- Theophel, K., Schacht, V. J., Schlüter, M., Schnell, S., Stingu, C. S., Schaumann, R., et al. (2014). The importance of growth kinetic analysis in determining bacterial susceptibility against antibiotics and silver nanoparticles. *Front. Microbiol.* 5, 544. doi: 10.3389/fmicb.2014.00544
- Vázquez, J. A., Durán, A., Rodríguez-Amado, I., Prieto, M. A., Rial, D., and Murado, M. A. (2011). Evaluation of toxic effects of several carboxylic acids on bacterial growth by toxicodynamic modelling. *Microb. Cell Fact.* 10, 100. doi: 10.1186/1475-2859-10-100
- Walsh, S. E., Maillard, J. Y., Russell, A. D., Catrenich, C. E., Charbonneau, D. L., and Bartolo, R. G. (2003). Activity and mechanisms of action of selected biocidal agents on Gram-positive and -negative bacteria. *J. Appl. Microbiol.* 94, 240–247. doi: 10.1046/j.1365-2672.2003.01825.x
- Yoshimatsu, T., and Hiyama, K. I. (2007). Mechanism of the action of didecyltrimethylammonium chloride (DDAC) against *Escherichia coli* and morphological changes of the cells. *Biocontrol Sci.* 12, 93–99. doi: 10.4265/bio.12.93
- Zhang, A., He, X., Meng, Y., Guo, L., Long, M., Yu, H., et al. (2016). Antibiotic and disinfectant resistance of *Escherichia coli* isolated from retail meats in Sichuan, China. *Microb. Drug Resist.* 22, 80–87. doi: 10.1089/mdr.2015.0061
- Zhang, C., Cui, F., Zeng, G. m., Jiang, M., Yang, Z. Z., Yu, Z. G., et al. (2015). Quaternary ammonium compounds (QACs): a review on occurrence, fate and toxicity in the environment. *Sci. Total Environ.* 518–519, 352–362. doi: 10.1016/j.scitotenv.2015.03.007
- Zou, L., Meng, J., McDermott, P. F., Wang, F., Yang, Q., Cao, G., et al. (2014). Presence of disinfectant resistance genes in *Escherichia coli* isolated from retail meats in the USA. *J. Antimicrob. Chemother.* 69, 2644–2649. doi: 10.1093/jac/dku197

Conflict of Interest: The authors declare that the research was conducted in the absence of any commercial or financial relationships that could be construed as a potential conflict of interest.

Publisher's Note: All claims expressed in this article are solely those of the authors and do not necessarily represent those of their affiliated organizations, or those of the publisher, the editors and the reviewers. Any product that may be evaluated in this article, or claim that may be made by its manufacturer, is not guaranteed or endorsed by the publisher.

Copyright © 2022 Pedreira, Vázquez and García. This is an open-access article distributed under the terms of the Creative Commons Attribution License (CC BY). The use, distribution or reproduction in other forums is permitted, provided the original author(s) and the copyright owner(s) are credited and that the original publication in this journal is cited, in accordance with accepted academic practice. No use, distribution or reproduction is permitted which does not comply with these terms.